Advanced Composite Materials
Publication details, including instructions for authors and subscription information:
http://www.tandfonline.com/loi/tacm20

Conductivity stability of carbon nanofiber/unsaturated polyester nanocomposites

Shi-Hong Wu [a] , Toshiaki Natsuki [b] , Ken Kurashiki [c] , Qing-Qing Ni [d] , Masaharu Iwamoto [e] & Yoshimichi Fujii [f]

[a] Division of Advanced Fibro-Science, Kyoto Institute of Technology, Matsugasaki sakyo-ku, Kyoto 606-8585, Japan
[b] Dept. of Functional Machinery and Mechanics, Shinshu University, 3-15-1 Tokida, Ueda 386-8567, Japan
[c] Division of Advanced Fibro-Science, Kyoto Institute of Technology, Matsugasaki sakyo-ku, Kyoto 606-8585, Japan
[d] Dept. of Functional Machinery and Mechanics, Shinshu University, 3-15-1 Tokida, Ueda 386-8567, Japan
[e] Division of Advanced Fibro-Science, Kyoto Institute of Technology, Matsugasaki sakyo-ku, Kyoto 606-8585, Japan
[f] Division of Advanced Fibro-Science, Kyoto Institute of Technology, Matsugasaki sakyo-ku, Kyoto 606-8585, Japan

Version of record first published: 02 Apr 2012.

To cite this article: Shi-Hong Wu , Toshiaki Natsuki , Ken Kurashiki , Qing-Qing Ni , Masaharu Iwamoto & Yoshimichi Fujii (2007): Conductivity stability of carbon nanofiber/unsaturated polyester nanocomposites, Advanced Composite Materials, 16:3, 195-206

To link to this article: http://dx.doi.org/10.1163/156855107781393777

Adv. Composite Mater., Vol. 16, No. 3, pp. 195–206 (2007)

Conductivity stability of carbon nanofiber/unsaturated polyester nanocomposites

SHI-HONG WU [1], TOSHIAKI NATSUKI [2], KEN KURASHIKI [1],
QING-QING NI [2], MASAHARU IWAMOTO [1] and YOSHIMICHI FUJII [1,*]

[1] *Division of Advanced Fibro-Science, Kyoto Institute of Technology, Matsugasaki sakyo-ku, Kyoto 606-8585, Japan*
[2] *Dept. of Functional Machinery and Mechanics, Shinshu University, 3-15-1 Tokida, Ueda 386-8567, Japan*

Received 6 July 2006; accepted 30 October 2006

Abstract—Carbon nanofiber (CNF)/unsaturated polyester resin (UPR) was prepared by a solvent evaporation method, and the temperature dependency of electrical conductivity was investigated. The CNF/UPR composites had quite a low percolation threshold due to CNF having a larger aspect ratio and being well dispersed in the UPR matrix. The positive temperature coefficient (PTC) was found in the CNF/UPR composites and it showed stronger effect around the percolation threshold. The electrical resistance of the CNF/UPR composites decreased and had lower temperature dependency with increasing numbers of thermal cycles.

Keywords: Carbon nanofiber; polymer; electrical properties; nanocomposites.

1. INTRODUCTION

Most pure polymers show electrical insulation properties. Electrical conductivity of insulating polymers can be achieved through incorporation of conductive fillers such as carbon black or metal powders into the polymer. The fillers come into contact with each other to form the conduction pathways through the resin matrix. The electrical resistivity of the composites, therefore, depends not only on the type of filler/polymer, but also on the dimension and distribution of filler [1–3].

An electrically conductive composite can be widely used for electric fields, such as static dissipative, semi-conductive, electromagnetic interference (EMI)/radio frequency interference (RFI) shielding, and positive temperature coefficient (PTC)

Edited by the JSCM.

[*] To whom correspondence should be addressed. E-mail: fujii@kit.jp

materials [4, 5]. Under joint action of electric field and/or varying temperature, the conductive stabilization of composites is quite important in the application fields. One important property of the electrically conductive composites is a non-linear PTC effect, that is, their resistivity sharply increases with increasing temperature beyond the range of the melting point or glass transition temperature. The mechanism has been explained by the increase of tunneling thickness or the breakdown of percolating network because thermal expansions have difference between the matrix and the filler with an increase of Joule heating or ambient environment temperature [6, 7].

In recent years, carbon nanofiber (CNF) has attracted great attention because of its excellent properties, such as high stiffness and strength, remarkable thermal and electrical conductions [8, 9]. Advantages of filled CNT composites as compared to metals include improved corrosion resistance, lighter weight, and the ability to adapt the conductivity properties to suit the needs of application. Vapor grown carbon fiber (VGCF) has been well known to exhibit good electrical conductivity compared to other types of carbon fibers [9]. Since they have a very small diameter, the VGCFs tend to have a larger aspect ratio than other general short carbon fibers. Therefore, the network of the nanofibers can be mass-produced, at low-cost and high efficiency, making them ideal for industrial applications. For example, as for the sheet shape exothermic body which possesses the PTC characteristics, it is possible to generate thermal runaway when the resistance value decreases rapidly due to softening of the resin with increasing temperature. Therefore, the stability of the conductive composite with the temperature change is of great importance. To the authors' knowledge, the conductivity stability of electrical resistivity for nanocomposites filled with CNFs is rarely investigated.

In the present work, the traditional solution evaporation method was not used for the reduction of environmental burden caused by organizational solutions. The carbon nanofiber (CNF)/unsaturated polyester resin (UPR) was prepared by a sonicated method. The electrical resistance of the composites as a function of CNF content was investigated so as to understand the percolation behavior, temperature-resistivity and current-voltage characteristics.

2. EXPERIMENTAL DETAILS

2.1. Materials

CNF used in this study was VGCF obtained from Showa Denko. Co. Ltd., Japan. The average diameter was about 150 nm and the length was 10–20 μm. The resin used as matrix was unsaturated polyester resin (UPR) and the hardening agent was PERMEK, produced by NOF Co., Ltd. The properties of CNF and UPR are listed in Table 1.

Table 1.
Properties of carbon nanofiber and unsaturated polyester resin

Properties	CNF	UPR
Density (g/cm^3)	2	1.016
Diameter (nm)	150	–
Length (µm)	20	–
Resistivity (Ω cm)	0.012	1.0×10^{14}
Coefficient of linear expansion (1/°C)	–	5.0×10^{-5}

2.2. Sample preparation

The nanocomposite sheets with different VGCF contents were prepared by the sonicated method. VGCF filler of several weight fractions were added to the unsaturated polyester resin and stirred well with a glass rod. Next, the composite slurry was ultrasonicated at 80°C for 3 h to homogenize it. Then, the hardening agent was added and a sheet with 1 mm thickness was formed at room temperature for 24 h. Furthermore, heat treatment was conducted at 100°C for 1 h in the drying oven.

2.3. Electrical resistivity measurement

The electrical resistivity was measured by a two-terminal method. The samples with rectangular shape ($20 \times 5 \times 1$ mm^3) were cut from the nanocomposite sheet. The surfaces of the specimens were coated with silver paste in order to ensure a good electrical contact resistance between the material surface and the copper electrodes. The electrical resistances of 5 samples for each fiber fraction were measured at room temperature, using a digital multi-meter VOAV7510 (Iwatsu Co. Ltd. Japan). For the electrical resistivity measurement in changing temperature, the specimen with the attached copper electrodes was placed in an oven where temperature was controlled in accordance with a desired program from room temperature to 200°C. The temperature dependency of the electrical resistance was measured at the heating rate of 2°C/min. The time dependency of the electrical resistivity was measured by using a direct current voltage source at a given annealing temperature of 190°C. Direct current was used to measure current-voltage characteristics at constant temperature and the voltage values were changed from 5 to 100 V.

2.4. Morphology observation

The morphology of the nanocomposites was observed using scanning electron microscopy S-510 (Hitachi, Co. Ltd. Japan). In order to clearly observe the surfaces and fracture surfaces, the samples were sputtered with gold.

3. RESULTS AND DISCUSSION

3.1. Morphology of nanocomposites

Figures 1(a) and 1(b) show SEM micrographs of the skin surface and fractured cross section of the UPR filled with 1 wt% and 4 wt% CNF, respectively. The darker regions in the images correspond to the UPR and the brighter regions to CNFs. The SEM images show smooth surface state in the nanocomposites. The observation indicates that there exists perfect adhesive property between the skin surface and the electrode with silver paste, and consequently contact resistance is decreased. Figures 1(c) and 1(d) show the SEM micrographs of the fracture surface of the UPR filled with 1 wt% and 4 wt% CNF, respectively. The slender and brighter regions in the images correspond to the CNFs. The SEM images show random and uniform dispersion of CNFs in the nanocomposites. The observation can prove that increasing physical contact between CNF and CNF results in an improvement in conduction characteristics of the nanocomposites.

Figure 2 shows the influence of CNF weight fraction on the volume electrical resistivity of the CNF/UPR nanocomposites. The electrical resistivity depends strongly on the CNF fraction. It is found that the variation of the resistance with the CNF fiber fraction exhibits a typical percolation behavior. A sharp drop is observed

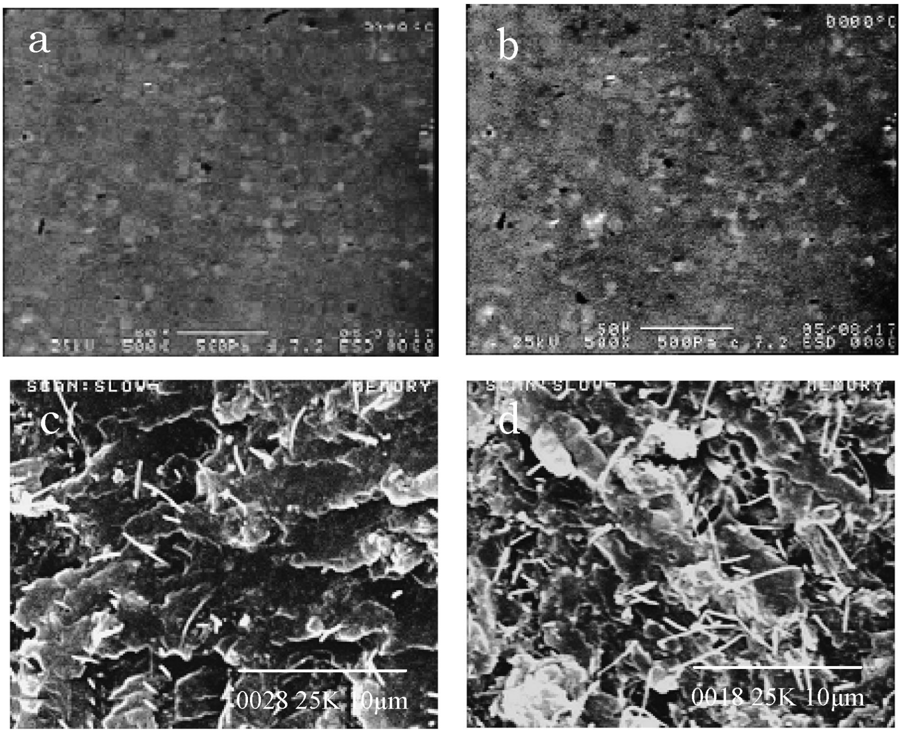

Figure 1. SEM micrographs of the skin surface and fractured cross section of unsaturated polyester resin filled with 1 wt% and 4 wt% CNF, respectively.

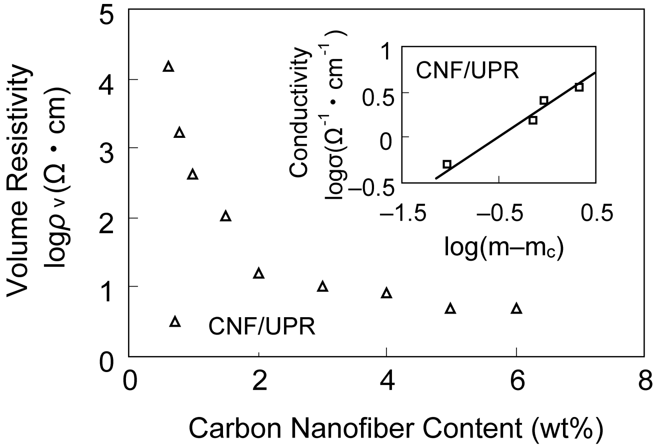

Figure 2. Relationship between electrical volume resistivity and CNF content for the CNF/UPR nanocomposites.

to between 2 wt% and 3 wt%, which shows that the CNF/UPR nanocomposites have a low percolation threshold. This is mainly because the CNF possesses larger aspect ratios and is well dispersed within the matrix, increasing physical contacts and conducting pathways between themselves. In addition, the polymer cannot completely wet the surface of the CNFs because of the lower wettability that is characteristic of the CNFs. The low resistance film can generate the percolative connectivity and results in a low resistance. On the other hand, the conducting pathways in nanocomposites filled with CNF are not only the physical contacts between themselves, but also the connections between the CNFs with very small intervals across which electrons can tunnel [10, 11].

In general, the electrical conductivity of nanocomposites satisfies a power law relation as [12]

$$\sigma \propto (m - m_c)^{\beta_c}, \quad m > m_c, \tag{1}$$

where σ is the electrical conductivity, m is the CNF mass fraction, m_c is the critical fraction corresponding to the percolation threshold, and β_c is the critical exponent, it represents only the universality classes like the dimensionality of the system. Based on the least square method, $\beta_c = 0.93$ is obtained from the experimental data shown in Fig. 2. The result suggests that a CNF network exists in CNF/UPR nanocomposites in which the CNFs contribute to conductive paths. The experimentally measured values of the critical exponent are close to, but somewhat lower than, other reported values. Different numerical approaches found universal critical exponent between 1.3 and 2 for a three-dimensional materials system. Indeed, non-universal values have been sometimes reported; therefore, the universality of the critical exponent is still controversial in conductive materials [8, 13, 14]. Such differences can be explained by differences in the method of formation that resulted in different dispersion states of the fiber and the contact resistance between fiber and fiber.

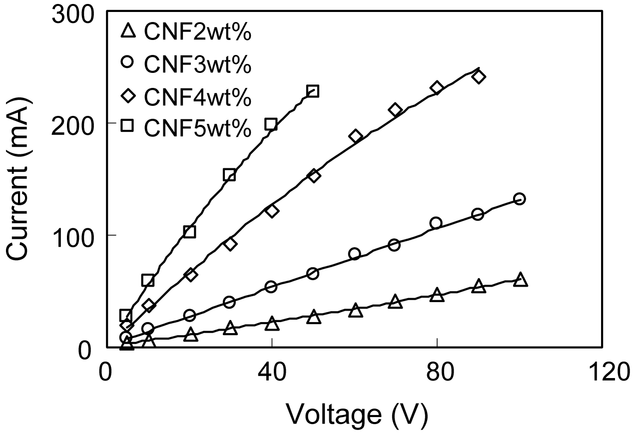

Figure 3. Relations between current and voltage for CNF/UPR nanocomposites.

3.2. Voltage-current characteristics

The current-voltage characteristics were studied for the nanocomposites with different content of CNFs. Figure 3 shows the current–voltage dependence of different CNF contents. The current–voltage behavior of the nanocomposites with 2–3 wt% CNF contents is almost linear relationship obeying Ohm's law. For the nanocomposites with 4–5 wt% CNF contents, the behavior of current–voltage is observed to be a slightly nonlinear relationship with increasing electric fields. This is because, with higher CNF fiber fraction, as the electric field is increased above a certain voltage (gate voltage), the higher current density leads to a decrease in nanocomposite resistance. The high current density rapidly generates the joule heating effect and consequently increases the sample temperature as well as decreases the current. Consequently, the current of the samples results in nonlinear increase with increasing voltage. This behavior suggested that the dominant conduction mechanism is conventional Ohmic conduction owing to the contact conductivity between CNFs [15−17]. This conclusion can also be drawn from the relationship between the characteristic resistivity and CNF contents shown in Fig. 2. The conductivity mechanism of nanocomposites exhibits Ohmic conduction when CNF contents are larger than around 2 wt%.

3.3. Temperature dependence of electrical resistivity

Figure 4 shows the temperature dependency of the electrical resistivity of CNF/UPR composites as a function of filler contents. The temperature dependency of the electrical resistivity can be expressed as [14, 18]

$$\rho_T = \rho_0 + A \exp[k(T - T_0)], \tag{2}$$

where ρ_0 is the nanocomposite resistivity at room temperature T_0, A is related to the contact resistance between adjacent carbon nanofibers, and k is the coefficient of

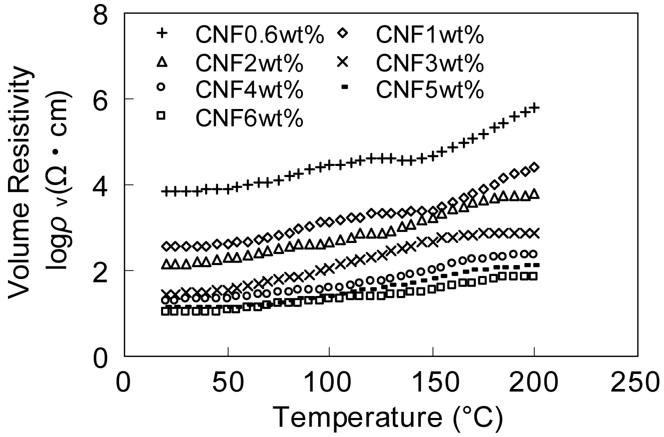

Figure 4. Temperature dependency of volume resistivity in CNF/UPR nanocomposites.

thermal expansion (CTE) for nanocomposites. The model describes a mechanism for tunneling of electrons through a barrier whose height is varying due to local temperature fluctuations. It is assumed that the two conducting islands separated by an insulating layer form a junction and charge carrier can tunnel through this junction. Based on this model, the resistance of the CNF/UPR nanocomposites is mainly composed of two parts: one is the resistance of CNF, and the other is the contact resistance between adjacent CNFs. Owing to the very large CTE of UPR matrix compared to CNF, the width of the gap between adjacent CNFs enlarges when the temperature is increased. The increasing distance hinders the process of electron tunneling, which results in the increase of the contact resistance and is responsible for the increased resistivity of nanocomposites when the temperature increases.

The negative temperature coefficient (NTC) effect was not observed in our work. This is because the NTC effect can be eliminated by the chemical crosslinking method. The crosslinking increases the viscosity of the matrix and produces a gel like network, resulting in the stabilization of conductive filler dispersion [7]. According to the widely accepted explanation reported in the literature [19, 20], thermosetting unsaturated polyester resin produces a reticulation network through thermal treatment of CNF/UPR nanocomposites, resulting in a restraint force against CNFs. In addition, it exhibits large adhesive force between CNFs and matrix because the very high surface-to-volume ratio of CNFs produces a strong interfacial bond. Based on the two explanations, the NTC effect could not be observed due to the stabilization of the CNF in the state of softening of polymer, and the formation of disconnected conductive pathways is scarcely to be observed under these conditions.

In order to examine how sensitive and to what extent the resistance response will be after being stimulated by the change in the temperature, the relative resistivity

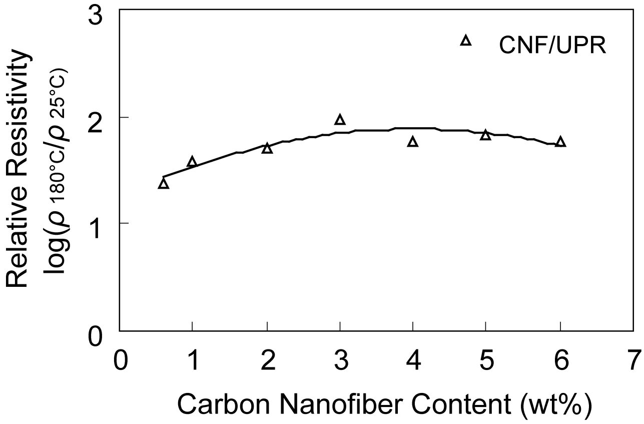

Figure 5. The effect of CNF content on the relative resistivity in CNF/UPR nanocomposites.

(ρ_r) can be defined as PTC intensity:

$$\rho_r = \log(\rho_{180^\circ}/\rho_{25^\circ}), \tag{3}$$

where ρ_{180° and ρ_{25° is the resistivity at 180°C and 25°C, respectively. The effect of CNF contents on the relative resistivity are shown in Fig. 5. The relative resistivity of CNF/UPR nanocomposites has the highest values around the critical volume fraction of 3 wt%. This result suggested the temperature dependence of the electrical resistance on CNF content is exhibited strongly near the percolation threshold. This is because the network of CNFs is at the critical state. This was easily fractured with the thermal expansion of composites, consequently resulting in the large change of the resistance.

3.4. Conducting hysteresis

In order to examine the reproducibility of the PTC effect and the conduction, the resistance measurement on several heating/cooling cycles was carried out. Figure 6 shows the temperature dependence of the resistance during the repeated heating/cooling cycling experiments for the nanocomposites with 3 wt% CNF content. The reproducibility of the PTC effect for CNF/UPR nanocomposites is poor because the change in the electrical resistivity decreases with an increase in cycling numbers. Especially, the temperature response of the electrical conductivity largely decreases after the first heating/cooling cycle. For the fourth and the fifth cycles, the electrical resistivity with the temperature (less than about 70°C) remains almost constant. The results indicated that the main reason for decreased resistance of nanocomposites is the result of improving degree of three-dimensional reticulation structure and the relaxation behavior of the residual stress, which produces a shrinkage of matrix volume after heating/cooling cycles. A new continuous conductive path is then established because the contact areas are increased among CNFs, which results in a decrease in the electrical resistance.

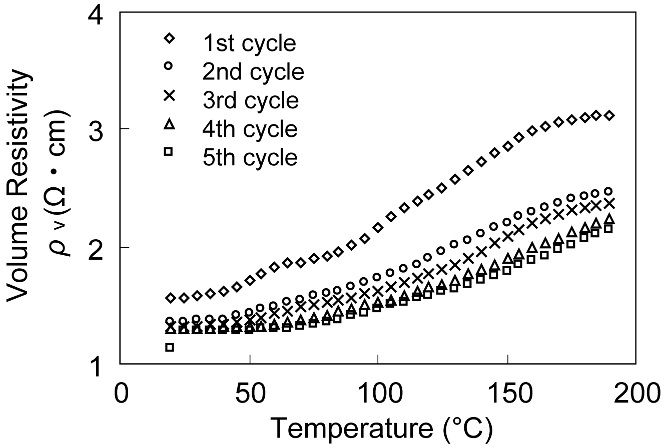

Figure 6. Temperature dependency of volume resistivity as a function of thermal cycle in CNF/UPR nanocomposites (3 wt% content CNF).

Moreover, Fig. 6 shows the decrease of temperature dependence of nanocomposites with increasing heating/cooling cycle times. The results can be explained by suggesting that the shrinkage of the matrix volume improved the hardening degree and changed the thermal viscoelastic characteristics. As a result, the coefficient of thermal expansion becomes rather small, resulting in decreasing of the temperature dependence.

3.5. Time dependence of the electrical resistivity

The conductive fillers move to coalesce in a way comparable to that of Brownian movement at high temperature beyond the glass transition temperature or the melting temperature of the polymer matrix, and finally form the three-dimensional conductive network by the isothermal treatment method [21]. Figure 7 shows the time dependence of the electrical resistivity for CNF/UPR nanocomposites with 3 wt% CNF content annealed at 190°C. It is observed that the initial resistivity of the nanocomposites drastically increases and reaches a maximum with increasing time. Then, the values decrease little and become approximately constant at a value that is higher than room-temperature resistivity. This phenomenon is believed to be closely associated with the matrix thermal expansion and polymer chains' relaxation behavior [22, 23]. Since the matrix rapidly expands when the temperature increases, the width of the conductive gaps increases, which inhibits electron tunneling and results in increased resistivity. When the thermal expansion becomes stable with increasing time, CNFs form a conductive network due to Brownian movement of the matrix, resulting in a decreased resistance, which becomes approximately constant. The direct current resistance (true resistance) mainly includes the resistance of the conductive filler and the resistance of the conductive filler boundary in conductive composites. In an alternating electric field, the speed of response of conduction is a measure of the difference for each resistant component. The lag of the phase occurs

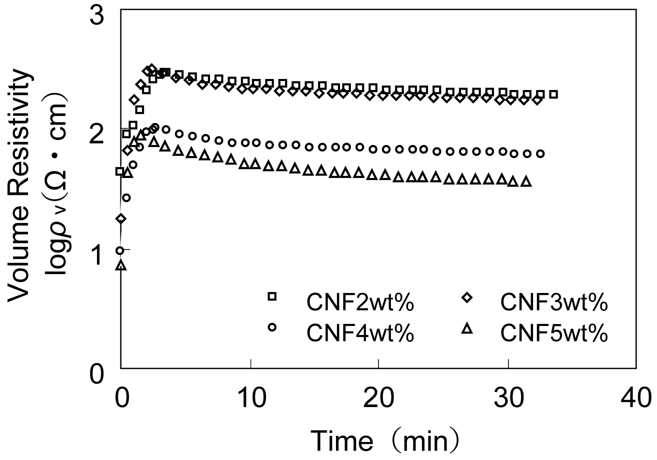

Figure 7. Time dependency of electrical volume resistivity for CNF/UPR nanocomposites at the ambient temperature 190°C.

between the response current and voltage with the change of frequency, and the reactance of the composites changes. Impedance of the composites (AC resistance) generally decreases with increase in the frequency [24, 25].

4. CONCLUSION

In this paper, the CNF/UPR nanocomposites are innovated by using directly mixed and sonicated methods, and their electrical properties are investigated as follows.

(1) The CNF/UPR nanocomposites materials exhibit a very low electrical percolation threshold because the CNF have not only a larger aspect radio but also a tunneling conductivity.

(2) The temperature dependency obeys the quantum tunnel model described by Sheng *et al.* [11]. The CNF/UPR nanocomposites are observed to have PTC effect since the thermal expansion coefficient of the UPR matrix is much lager than that of the CNFs, resulting in the width of the gap between contiguous CNF becoming enlarged. Moreover, the PTC effect depends on CNF contents and the temperature dependence of the PTC near the percolation threshold has a stronger influence than that of other contents.

(3) The PTC effect and volume resistivity decrease with increase in the thermal/cooling cycle number due to changing of the thermal viscoelastic characteristics (improving of hardening degree) and the relaxation behavior of the residual stress of the resin matrix.

REFERENCES

1. Y. H. Hou, M. Q. Zhang and M. Zh. Rong, Performance stabilization of conductive polymer composites, *J. Appl. Polym. Sci.* **89**, 2438–2445 (2003).
2. W. H. Di and G. Zhang, Resistivity-temperature behavior of carbon fiber filled semicrystalline composites, *J. Appl. Polym. Sci.* **91**, 1222–1228 (2004).
3. Ch. Ch. Ma, Y. L. Huang, H. C. Kuan and Y. S. Chiu, Preparation and electromagnetic interference shielding characteristics of novel carbon-nanotube/siloxane/poly-(urea urethane) nanocomposites, *J. Polym. Sci.: Part B: Polym. Phys.* **43**, 345–358 (2005).
4. N. B. Janda, J. M. Keith, J. A. King, W. F. Perger and T. J. Oxby, Shielding-effectiveness modeling of carbon-fiber/nylon-6,6 composites, *J. Appl. Polym. Sci.* **96**, 62–69 (2005).
5. S. Shekhar, V. Prasad and S. V. Subramanyam, Transport properties of conducting amorphous carbon/poly(vinyl chloride) composite, *Carbon* **44**, 334–340 (2006).
6. F. Carmona and C. Mouney, Temperature-dependent resistivity and conduction mechanism in carbon particle-filled polymers, *J. Mater. Sci.* **27**, 1322–1326 (1992).
7. C. Zhang, C. A. Ma, P. Wang and M. Sumita, Temperature dependency of electrical resistivity for carbon black filled ultra-high molecular weight polyethylene composites prepared by hot compaction, *Carbon* **43**, 2544–2553 (2005).
8. B. Kin, J. Lee and I. Yu, Electrical properties of single-wall carbon nanotube and epoxy composites, *J. Appl. Phys.* **94**, 6724–6728 (2003).
9. J. Xua, J. P. Donohoeb and C. U. Pittman Jr., Preparation, electrical and mechanical properties of vapor grown carbon fiber (VGCF)/vinyl ester composites, *Composites: Part A* **35**, 693–701 (2004).
10. D. Toker, D. Azulay, N. Shimoni, I. Balberg and O. Millo, Tunneling and percolation in metal-insulator composite materials, *Phys. Rev. B* **68**, 041403-1 (2003).
11. P. Sheng, E. K. Sichel and J. I. Gittleman, Fluctuation induced tunneling conduction in carbon polyvinylchloride composites, *Phys. Rev. Lett* **40**, 1197–1200 (1978).
12. F. Du, R. C. Scogna, W. Zhou, S. Brand, J. E. Fischer and K. I. Winey, Nanotube networks in polymer nanocomposites: rheology and electrical conductivity, *Macromolecules* **37**, 9048–9055 (2004).
13. F. Dalmas, R. Dendievel, L. Chazeau, J. Cavaille and C. Gauthier, Carbon nanotube-filled polymer composites. Numerical simulation of electrical conductivity in three-dimensional entangled fibrous networks, *Acta Materialia* **54**, 2923–2931 (2006).
14. J. M. Benoit, B. Corraze and O. Chauvet, Localization, Coulomb interactions, and electrical heating in single-wall carbon nanotubes/polymer composites, *Phys. Rev. B* **65**, 241405(1)–241405(4) (2002).
15. Y. Chekanov, R. Ohnogi, S. Asai and M. Sumta, Electrical properties of epoxy resin filled with carbon fibers, *J. Mater. Sci.* **34**, 5589–5592 (1999).
16. H. Bar, M. Narkis and G. Boiteux, The electrical behavior of thermosetting polymer composites containing metal plated ceramic filler, *Polym. Compos.* **26**, 12–19 (2005).
17. F. El-Tantawy, New double negative and positive temperature coefficients of conductive EPDM rubber TiC cerimic composites, *Eur. Polym. J.* **38**, 567–577 (2002).
18. X. Liang, The dependence of resistivity of carbon fibers/ABS resin composites on the temperature, *J. Mater. Sci. Lett.* **19**, 1215–1216 (2000).
19. J. C. Lee, K. Nakajima, T. Ikehara and T. Nishi, Conductive-filler-filled poly(1-caprolactone)/poly (vinylbutyral) blends. II. Electric properties (positive temperature coefficient phenomenon), *J. Appl. Polym. Sci.* **65**, 409–416 (1997).
20. W. Di, G. Zhang, J. Q. Xu, Y. Peng, X. J. Wang and Z. Y. Xie, Positive-temperature-coefficient/negative-temperature-coefficient effect of low-density polyethylene filled with a mixture of carbon black and carbon fiber, *J. Polym. Sci.: Part B: Polym. Phys.* **41**, 3094–3101 (2003).

21. G. Wu, T. Miura, S. Asai and M. Sumita, Carbon black-loading induced phase fluctuations in PCDF/PMMA miscible blends: dynamic percolation measurements, *Polymer* **42**, 3271–3279 (2001).
22. C. Zhang, P. Wang, C. Ma, G. Wu and M. Sumita, Temperature and time dependency of conductive network formation: dynamic percolation and percolation time, *Polymer* **47**, 466–473 (2006).
23. A. Katada, Y. Konishi, T. Tominaga, S. Asai and M. Sumita, Dynamic percolation phenomenon of poly(methyl methacrylate)/surface fluorinated carbon black composite, *J. Appl. Polym. Sci.* **89**, 1151–1155 (2003).
24. J. M. Torrents and T. O. Mason, Analysis of the impedance spectra of short conductive fiber reinforced composites, *J. Mater. Sci.* **36**, 4003–4012 (2001).
25. J.-E. Park, M. Saikawa, M. Atobe and T. Fuchigami, Highly-regulated nanocoatings of polymer films on carbon nanofibers using ultrasonic irradiation, *Chem. Commun*. 2708–2710 (2006).